Diffusion Kurtosis Imaging and Pathology in Spinal Cord Ischemia/Reperfusion Injury in Rabbits: A Case-Control Study

Authors' Contribution:
Study Design A
Data Collection B
Statistical Analysis C
Data Interpretation D
Manuscript Preparation E
Literature Search F
Funds Collection G

ABCDEFG 1,2 **Daowei Li**
ABCDEFG 1 **Xiaoming Wang**

1 Department of Radiology, Shengjing Hospital of China Medical University, Shenyang, Liaoning, P.R. China
2 Department of Radiology, The People's Hospital of China Medical University and The People's Hospital of Liaoning Province, Shenyang, Liaoning, P.R. China

Corresponding Author: Xiaoming Wang, e-mail: wangxm024@163.com
Source of support: This work was supported in part by a grant from the Shengjing Free Researchers Fund (No. 2008-02), Shenyang City, China

Background: The aim of this study was to evaluate the application of diffusion kurtosis imaging (DKI) in spinal cord ischemia/reperfusion (SCI/R) injury and to explore its association with pathology.

Material/Methods: Japanese male long-eared rabbits were chosen and divided into 7 groups (8 rabbits in each group): control group (C group), sham-operation control group (S group), and 5 experimental groups (E-2 h group, E-24 h group, E-48 h group, E-7 d group, and E-14 d group). Tarlov scoring and immunohistochemical staining were used to assess hindlimb motor function and observe the expression of glial fiber acidic protein (GFAP), respectively. The correlation between DKI and pathology after SCI/R injury was compared by 3.0TMR scanning DKI.

Result: Neuroethology in each time point of E groups was significantly different from that in C and S groups ($P<0.05$). The E-24 h group had the lowest value ($P<0.05$), and the hindlimb motor function began to recover after 24 h. The expression of GFAP was gradually increased after SCI/R injury, and the maximum value was in the E-7 d group ($P<0.05$). MK (mean kurtosis) had a linear negative correlation with average optical density (OD) ($r=-0.115$, $P<0.05$) and was positively correlated with integral OD (IOD) ($r=0.204$, $P<0.05$), in which MD (mean dispersion) was positively correlated with OD and IOD, but without a significant difference ($r=0.618$, $r=251$, $P>0.05$).

Conclusions: DKI can be used to monitor the changes in SCI/R injury, and fractional anisotropy (FA) can reflect change in white matter structure. The changes in expression of MK and GFAP were related to the myelin sheath injury repair process.

MeSH Keywords: **Diffusion Magnetic Resonance Imaging • Hypoxia-Ischemia, Brain • Spinal Cord Injuries**

Full-text PDF: https://www.medscimonit.com/abstract/index/idArt/902986

📄 3467   ▦ 1   📊 6   📖 26

Background

Spinal cord ischemia/reperfusion (SCI/R) injury is an important factor in spinal cord injury [1]. The ability of myeloid tissue to tolerate ischemia and hypoxia is poor. If blood reperfusion is used after spinal cord injury, short-term neurological symptoms can be improved. However, the original injury can further aggravate and cause secondary damage, or even paraplegia, with prolongation of reperfusion [2]. The specific mechanism of SCI/R injury is not completely clear, and its incidence is increasing yearly [3]. There is no effective treatment at present [2]. When the spinal cord is damaged, ischemia can stimulate mature astrocytes to synthetize glial fiber acidic protein (GFAP), which is mainly used to mark glial activity after injury. Increased levels of GFAP-positive astrocytes after injury can promote the mitosis of astrocytes, which makes the primitive progenitor cells differentiate into mature astrocytes [4]. Many neurotrophic factors can be released during the pyrolysis process of astrocytes, which can promote repair of the injured spinal cord. GFAP, as a marker of astrocytes, has been widely recognized [3], but at present it is not possible for a neurologic exam to predict the potential for axon and myelin injury [5].

Conventional MRI is not sensitive enough to the early stage of lesion-formation, and the correlation with clinical symptoms is poor. Functional evaluation of spinal cord injury mainly relies on the subjective judgment of clinicians and lacks objective imaging criteria. Diffusion kurtosis imaging (DKI) is a non-invasive MRI technology used to detect the microstructure of tissue in vivo [6]. Based on the non-Gaussian motion model, the apparent diffusivity (Dapp) and the apparent kurtosis (Kapp) were used as 2 parameters to describe the diffusion of water molecules [7]. Thus, DKI is more accurate than diffusion tensor imaging (DTI) to describe the limited extent and heterogeneity of the diffusion [4], which can further evaluate the dynamic micro-structures such as spinal cord neurons and nerve fibers, damage, regeneration, and repair [8].

Research on SCI/R injury has become a popular research topic in recent years, but there has been relatively little research on use of DKI in SCIR injury, which is still in the laboratory and preliminary clinical research stages. Appling DKI to the rabbit ischemia reperfusion model, this study assessed the correlation between pathological changes and DKI diffusion parameters, providing an imaging standard for protective measures after spinal cord injury.

Material and Methods

Grouping of experimental animals

This study was approved by the Ethics Committee at our hospital (No. 2015PS233K) and was conducted in accordance with the provisions of the Declaration of Helsinki, Good Clinical Practice guidelines, and local laws and regulations.

We obtained 56 Japanese male long-eared rabbits (weight: 2.0–2.5 kg) from the Animal Experimental Center of our hospital. Rabbits were sub-cage reared 7 days and fasted 8 h before the experiment at 20–22°C, and then divided into 7 groups (8 rabbits in each group): control group (C group), sham-operation control group (S group), and 5 experimental groups (E groups) including E-2 h group, E-24 h group, E-48 h group, E-7 d group, and E-14 d group [9]. In the S group, we only exposed the infrarenal abdominal aorta after opening the abdominal cavity without occluding, the E group received the classic ischemic treatment [10], and the C group did not receive any treatment.

Establishment of the ischemia/reperfusion model

Rabbits were intramuscularly anesthetized with 20 mg/kg ketamine and monitored by ECG; a venous channel was established in the left ear margin. An abdominal incision was made 3 cm below the xiphoid and 6 cm above the pubis. Each layer of the abdominal wall was cut; the intestine tube was pushed gently to the right and covered with a warm gauze pad infiltrated with physiological saline. The left renal artery and about 1.5 cm of the abdominal aorta were exposed and freed. After 1 mg/kg heparin was given intravenously for 5 min, the abdominal aorta was occluded by a clamp at the L3 vertebral body level and 1 cm below the open of left renal artery for 25 min, then opened and reperfused for 1 min. One min occluding and 1 min opening was set as a cycle, and 5 cycles were given to make the ischemia/reperfusion model. After the cycles, the clamp was removed to observe the vascular filling status. The abdominal cavity was confirmed to be without capillary hemorrhage and was washed with 10 ml metronidazole and 80 000 U gentamicin, and then the abdominal wall was closed [10].

MRI scanning and image processing

After rabbits were anesthetized in total sleep, they were placed on their backs and fixed on a flat plate to keep the head in the same line as the spine. We used 3.0T (Ingenia; Philips Medical Systems, Best, Netherlands) to scan the L3-S1 vertebral body level with an 8-channel head and neck combined coil. Indexes were: Respiratory control mode, SE echo-planar imaging (EPI) sequence, 1 mm depth; T1WI (TR 510 ms, TE 11 ms), T2WI (TR 1.5 s, TE 100 ms), FOV 130 mm×130 mm^2; DKI sequence (TR 2.0 s, TE88 ms, b=0, 1000, 2000, motion probing gradient (MPG) 25 directions, FOV 100×100 mm, matrix 128×l28, 2.0 mm depth. The gradient length (δ) was 7.2 and the time between the 2 leading edges of the diffusion gradient (Δ) was 18.2 ms. Data were processed by DKI software in a Philips EWS workstation. The T2WI sagittal plane in the L3–S1 vertebral body was located and the region of interest (ROI) was set in the

corresponding axis of the spinal cord. The ROI was 2.0 mm^2 and measured 3 times for an average. Image evaluation was performed independently by 2 senior experts.

Neurological score

Tarlov scoring was used to immediately assess the hindlimb motor function when rabbits were fully awake [11]. The scores were evaluated by 2 animal laboratory researchers and recorded by double-blind method.

Collection and staining of specimen

In accordance with ethics standard, rabbits were sacrificed 48 h after reperfusion and L3–S1 vertebral bodies were removed. After fixing for 48 h, myeloid tissue was stained. Myeloid tissue was fixed with 4% paraform for more than 48 h and washed for more than 30 min. We performed through dehydration with different concentrations of alcohol, transparency with xylene, wax dipping, embedding, and 5-μm paraffin sections were made.

After conventional HE staining, paraffin sections were observed under a light microscope (BA400, Thermo, USA). A continuous transverse view of the spinal cord was observed [10], which included the center of spinal cord injury, head 10 mm and end 10 mm, in a total of 6 sections. The normal neuron is polygonal in structure and has a clear cell nuclear structure with Nissl body [12,13]. The counting method is 3 continuously collected views along the axis from the periphery to the center, in which the axis is a straight line connecting the middle point of the central tube with the top of the anterior horn [12,13]. One of the anterior horns was randomly chosen with double-blind method by 2 pathology professionals, and the neurons were counted under the light microscope (BA400, Thermo, USA) and recorded.

GFAP in myeloid tissue was extracted. After warming for 30 min, the spinal cord biopsy specimen section was washed with phosphate-buffered solution (PBS) 3 times (5 min/time), incubated with 3% hydrogen peroxide at room temperature for 20 min, blocked with 10% normal goat serum at room temperature for 30 min, incubated with the first antibody (GFAP polyclonal antibody, 1: 400, Abcam, UK) overnight at 4°C, incubated with the secondary antibody (Goat Anti-Mouse/Rabbit,1: 400, KeyGEN BioTECH, China), colored with a 3'-methyl-dimethylaminoazobenzene (DAB) Kit (ZSBG-BIO, Beijing, China), and mounted with methylbenzene after dehydration. The positive expression of GFAP was that the growth cone of the neuron cell body was a brown-yellow protuberance, or plasma red stain [12]. Optical density (OD) of 3 views in each group was assessed by use of a Nikon Ni-E microscope (DS-Ri2, Nikon, Japan).

A section in each group was randomly selected for Luxol fast blue (LFB) staining [14]. After placing in an ethanol and chloroform solution (1: 1), the section was placed in 95% ethanol for 5 min, 0.1% Luxol Fast Blue at 56°C for 2 h, 95% ethanol for 5 min, 70% ethanol for 3 min, double-distilled water for 3 min, differentiated in 0.05% lithium carbonate solution for 10 min and 70% ethanol for 30 s, washed with double-distilled water until there was clear gray matter and white matter boundaries, and mounted with neutral balsam after washing with ethanol and dehydration. The normal LFB staining was that the normal structure of myeloid tissue and cortical and white matter showed clearly, the structure of myelin was compact with distinguished gray matter and white matter, and the nucleus of the neuron and colloid was bright blue. Integral optical density (IOD) was assessed and analyzed by Image-Pro Plus software (Image-Pro-Plus 6.0; Media Cybernetics, Silver Spring, MD).

Statistical analysis

SPSS 19.0 software was used to analyze data. All data are expressed as $\bar{\chi}\pm s$. The SNK test and non-parametric rank sum test (Kruskal-Wallis test) were used to comparison the average number. One-way ANOVA and Pearson correlation analysis were used to compared data from 2 groups. P values less than 0.05 were considered significant.

Results

MRI images of each group are shown in Figure 1. FA (fractional anisotropy) and MK (mean kurtosis) in the E group were lower than in the C group (P<0.05) and the overall trend was gradually decreasing. Compared with other groups, MK in the E-24 h group and E-24 h group was significantly difference (P<0.05). MD (mean dispersion) showed a gradual increasing trend, but the difference was not statistically significant (P>0.05, Figure 2).

In neurological scoring, each time point of the E group was significantly different from that of the C and S groups (P<0.05, Table 1), but there was no significant difference between the C and the S groups. After SCI/R injury, Tarlov scoring decreased and was the lowest in the E-24 h group. With the prolongation of reperfusion time, the damage was gradually reduced, and hindlimb motor function was partially recovered after 48 h of reperfusion (P<0.05). Eight rabbits in the E group developed paraplegia (1 in the E-2 h group, 3 in the E-24 h group, 2 in the E-48 h group, 1 in the E-7 d group, and 1 in the E-14 d group); the paraplegia rate was 14.3% and the recovery rate of hindlimb function was 85.7%.

Neurons were integrated and cells were polygonal in structure with clear nucleus structure in C and S groups (Figure 3A, 3B). The number of normal neurons in the E group was obviously lower than in the C and S groups, with statistically significant
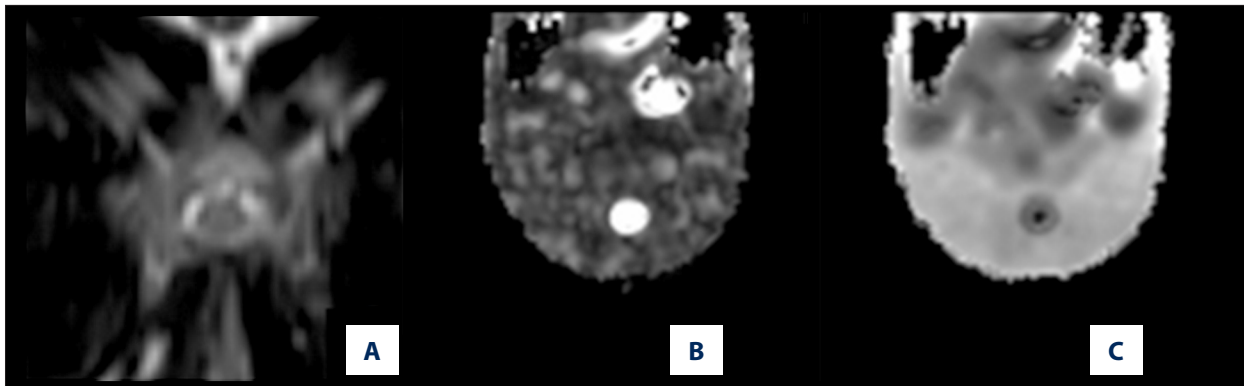
Figure 1. Spinal cord image of normal rabbit (**A**: T2WI axis, **B**: FA image, **C**: MK image).
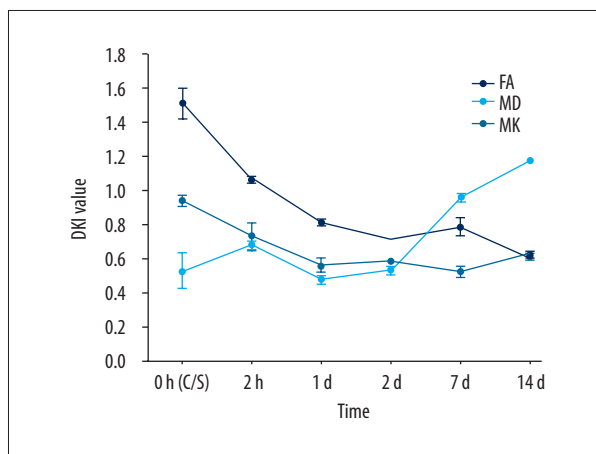

Figure 2. Trend chart of DKI parameter value (FA, MD, MK) in each group.

difference ($P<0.05$). With prolonged SCI/R time, the normal neurons in the anterior horn of the spinal cord decreased gradually, and were lowest at 14 d (Table 1).

In each group, astrocytes were found in the gray matter and white matter of the spinal cord, and the gray matter areas were more obvious (Figure 4). GFAP of the C and S groups was less, mainly distributed in the cytoplasm and star-shaped protuberances with small cell body and slender protuberance, which was significantly lower than in the E group ($P<0.05$, Figure 4A, 4B). The number of GFAP-positive cells increased in the E-2 h group,

with some irregular cell morphology, but there was no significant difference between the C and S groups ($P>0.05$, Figure 4C). The staining intensity of single positive cells and the total area of positive materials increased with time. GFAP-positive cells peaked at 7 d (Figure 4F).

LFB staining was similar in the C and S groups, in which the nerve fiber, myelin and axonal structure were complete, closely arrangement, the gray matter was almost clear, and the white matter was dark blue with a clear boundary (Figure 5A, 5B). The blue of the myelin was mostly light in the E-24 h group, and the nerve fibers were obviously decreased. IOD in each time point of the E group was less than in the C and S groups ($P<0.05$) and the lowest value 260.08 ± 9.35 appeared in the E-24 h group, which was obviously lower than in the other groups ($P<0.05$). IOD increased gradually, but there was no significant difference among the 48 h–14 d groups ($P>0.05$).

FA with a decreasing trend was not significantly different between the E group and the C group ($P>0.05$, Figure 6). FA in the E group was negatively correlated with OD ($r=-0.413$, $P<0.05$, Figure 6), and positively correlated with IOD ($r=0.121$, $P<0.05$, Figure 6), which was the same in MK ($r=-0.115$, $P<0.05$; $r=0.204$, $P<0.05$). MK in the E-24 h group and E-7 d group were significantly different from that in other groups ($P<0.05$) MD was positively correlated with OD and IOD, but there was no significant difference ($r=0.618$, $r=251$).

Table 1. Tarlov scoring and neurological scoring of each group(n=8).

	C group	S group	E group				
			2 h group	24 h group	48 h group	7 d group	14 d group
Tarlov Scoring	4±0	4±0	2.27±0.33	2.04±0.24	2.85±0.37	3.14±0.40	3.21±0.35
Neurological scoring	14.15±1.36	14.09±1.61	11.75±1.45	8.12±1.86	6.5±1.24	3.75±1.63	3.58±1.84

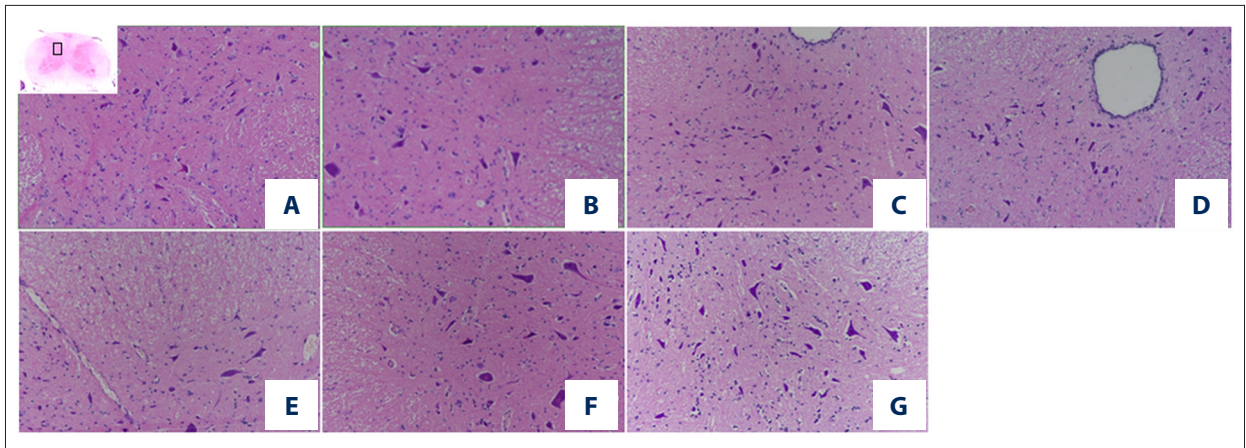* C group was control group; S group was sham-operation control group, E group was experimental group.

Figure 3. Histological changes after spinal cord ischemia/reperfusion injury in each group (HE staining, ×200). * **A** was control group; **B** was sham-operation control group, **C–G** was E-2 h group, E-24 h group, E-48 h group, E-7 d group, and E-14 d group.
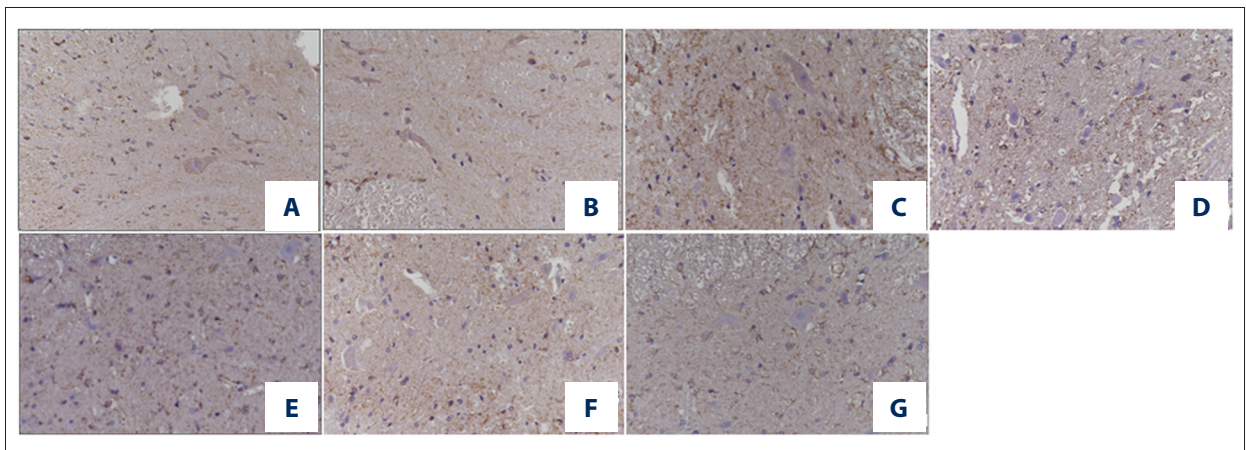

Figure 4. GFAP expression at different time points after spinal cord ischemia/reperfusion injury in rabbits (immunohistochemical staining, ×400). * **A** was control group; **B** was sham-operation control group, **C–G** was E-2 h group, E-24 h group, E-48 h group, E-7 d group, and E-14 d group.

Figure 5. Luxol fast blue staining after ischemia/reperfusion injury (LFB, ×400) * **A** was control group; **B** was sham-operation control group, **C–G** was E-2 h group, E-24 h group, E-48 h group, E-7 d group, and E-14 d group.
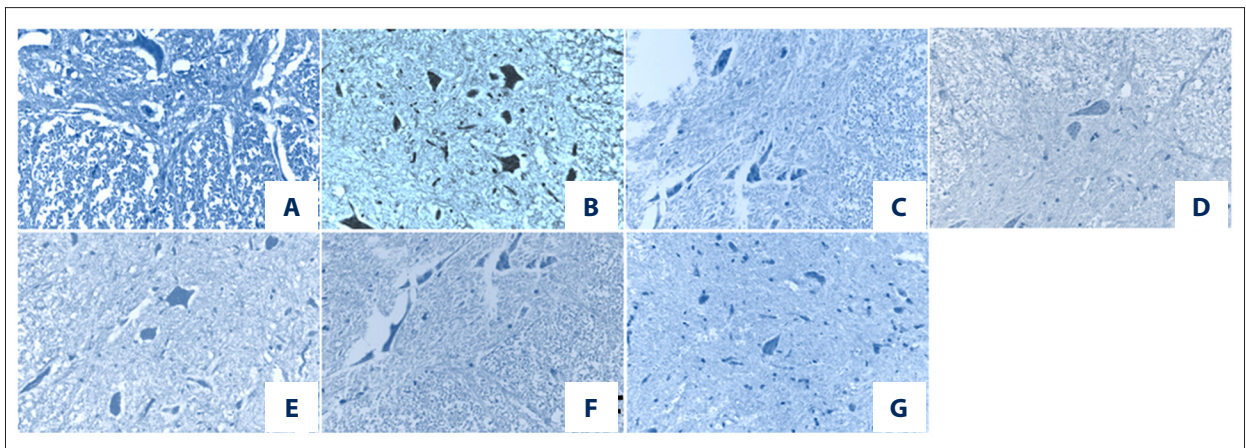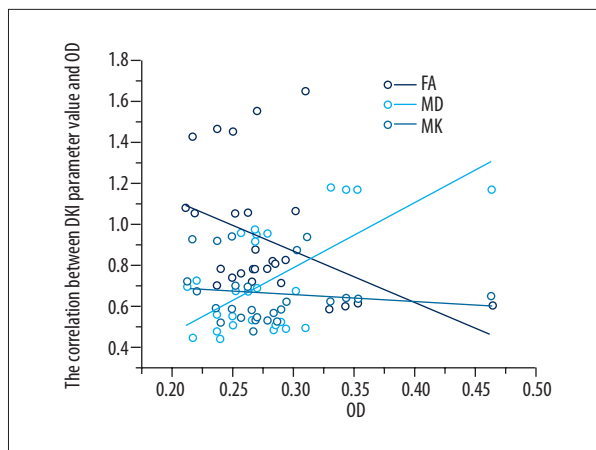
Figure 6. Correlation between DKI parameter value (FA, MD, MK) and optical density.

Discussion

In recent years, there has been increased research on regeneration and repair after SCI/R injury based on the reliable and reproducible SCI/R animal model [3]. Animal experiments show that it is possible to retain some important nerve function as long as 1.4~12% of axons remain in the spinal cord injury site [15]. Therefore, the clear mechanism of injury, the protective function of the organization, and early intervention can reduce the degree of spinal cord injury, decreasing the emergence of paraplegia and other complications [16].

Zivin [17] established the classical rabbit SCI/R injury model by directly occluding the infrarenal abdominal aorta, which is one of the main experimental methods used at present [17]. Spinal cord blood vessels of the long-eared rabbit are distributed segmentally with poor collateral circulation, making it easy to cause ischemia. Moreover, pathological changes in the ischemia model are consistent and reproducible. Sribnick et al. indicated that the MRI images of long-eared rabbits is similar to those of humans [18]. Previous SCI studies often ignored the delay of low perfusion after reperfusion and caused the secondary spinal cord damage [17]. After SCI, the degree of damage in the second paralysis in the hindlimbs was positively correlated with time [19], which was the same as in our study. Tarlov scoring in each time point of the E group was lower than that in the C and S groups (P<0.05, Table 1 and Figure 2), and the lowest value appeared in the E-24 h group (2.00±0.71), indicating that the second spinal cord injury can be caused after spinal cord reperfusion with an increasing trend in 24 h and then decreasing or becoming stable. The total paraplegia rate in this study was about 28% and the recovery rate was about 72%, which is consistent with the study by Zivin et al. [17], showing that the animal model was successfully established and could be further analyzed by pathology and imaging.

In SCI/R, microvascular permeability increased with dropsical neurons and glia cells [9,20]. With the prolongation of reperfusion time, the swelling of the anterior horn neurons gradually increased the necrosis. In this study, neurons in the E group showed pyknic or dissolved nuclei, eosinophilic-stained cytoplasm, unclear structure of nuclear membrane, dissolved myelinated nerve fiber, hemorrhage and necrosis of cells, and gradually reduced normal neurons in the anterior horn. Zivin et al. showed that spinal cord injury was most serious at the 24th hour (glial cells necrosis, disintegration, sparse neurons), the proportion of abnormal neurons increased [17], and was basically the same as the pathological changes found in the present study.

After SCI/R, the cells around the injured site undergo secondary damage, and can trigger apoptosis by the caspase pathway [21]. Oligodendrocytes in the spinal cord are very vulnerable to influence by apoptosis and lose the protective and supportive effect on the nerve cells. Induction in the immature stage and inhibition in the mature stage both can form astrocytes. In the immature stage, the hyperplasia of astrocytes is active and astrocytes can secrete glial cell line-derived neurotrophic factor, supporting and inducing nerve fiber regeneration. Glial scar formation has a mechanical barrier to nerve regeneration in the mature stage [22,23]. After SCI/R, the expression of GFAP gradually increased, reached a peak at 7 d (P<0.05), and then decreased gradually during 7 d to 14 d in our study, indicating that astrocytes are in immature stage during the early stage of injury, promoting the growth of neurons and elongating the axons, which cause the recovery of hindlimb function. Along with the proliferation and maturation of astrocytes, the glial scar formed and hindered the regeneration of nerves, inhibiting the further recovery of the hindlimb function. The same results were also reported by Hinkle et al. [24].

Myelin is a layer of insulating film wrapped around the outside of the nerve cell axon, which is composed of Schwann cells and myelin membrane. The damaged changes of myelin after SCI/R were observed by LFB staining. The lightest myelin staining appeared in the E-24 h group with serious dehydration, and with the prolongation of reperfusion the blue of myelin was gradually restored. The E-14 d group was deeper than the E-24 h group, but still lighter than the C and S groups.

There was no significant difference in FA between each time point of the E group and the control group (P>0.05), but there was a tendency to decrease. After myelin injury, the cell membrane structure was damaged and the structure of white matter pathways was changed continually, increasingly limiting the degree of diffusion of water molecules. The decreased FA could reflect the structural changes after white matter damage [25], but there was not statistically significant correlation with GFAP expression due to the small sample size and short

observation time. The study found that FA was more sensitive than MD and MK for observing the microstructure of the white matter [23].

After spinal cord injury, nerve fibers were demyelinated and axons were damaged, leading to increased extracellular volume, a significant decrease in FA, and increase in MD. In addition, intracellular abnormalities, such as cell debris, inflammatory, gliosis and other factors, will further restrict the isotropy of water molecules, resulting in the reduction of FA [8]. Although MD at each time point of the E group had an increasing trend, there was no significant difference in this study, perhaps because of the sample size or because the error leading to MD cannot accurately reflect the average diffusion of water molecules.

Biological diffusion of water molecules is subject to various restrictions and is not completely free. The degree of displacement and distribution that deviates from the Gaussian curve is called diffusion kurtosis (dimensionless), and its value reflects the complexity of organizational structure. MK is the average value of diffuse kurtosis along the direction of space in organization, in which greater MK indicates the more serious limitation, the more complex composition and structure, and is the most commonly used parameter in DKI clinical scientific research [8]. In this study, MK in each time point of the E group showed a decreasing trend with significant difference compared with the C group (P<0.05). MK and OD showed a negative linear correlation (r=−0.115, P<0.05) and a positive linear correlation with IOD (r=0.2.04, P<0.05). The E-24 h group and E-7 d group were significantly different from other groups (P<0.05). After SCI/R, cell membranes ruptured, the GFAP expression increased, some of the myelin of nerve fibers were damaged, and the complexity of the tissue structure decreased with relative decreasing MK. During 7 d to 14 d period, tissue necrosis, cavity formation, peripheral glial scar proliferation,

and blocked GFAP expression all lead to the slow change trend of MK. Related studies also showed that the decrease of MK not only reflects the influence of the microcirculation obstacle on the neurons and axons of spinal cord gray matter, but also reflects the direction of the white matter pathways and the degree of repair of myelin damage [26]. Due to the small sample size and the selected time points, this study cannot fully explain the correlation between DKI parameters and pathology. In subsequent research, we will increase the sample size and the selected time points, especially during the 1-day to 2-day period, to provide a more accurate time window for clinical treatment and avoid serious complications after SCI/R injury.

Conclusions

The SCI/R injury model was successfully established in this study and the study confirmed that DKI can predict changes in SCI/R spinal cord injury. FA can reflect the change of the white matter pathways structure. MK was related to the expression of GFAP and the repair process of myelin injury, which supports clinical early assessment and early intervention to avoid or reduce the emergence of irreversible changes in tissue.

Acknowledgements

Conflict of interest statement

The authors declare no conflict of interest in preparing this article.

References:

1. Mondal S, Dirks P, Rutka JT: Immunolocalization of fascin, an actin-bundling protein and glial fibrillary acidic protein in human astrocytoma cells. Brain Pathol, 2010; 20: 190–99

2. Kakimoto M, Kawaguchi M, Sakamoto T et al: Evaluation of rapid ischemic preconditioning in a rabbit model of spinal cord ischemia. Anesthesiology, 2003; 99: 1112–17

3. Lee BB, Cripps RA, Fitzharris M, Wing PC: The global map for traumatic spinal cord injury epidemiology: Update 2011, global incidence rate. Spinal Cord, 2014; 52: 110–16

4. Hori M, Tsutsumi S, Yasumoto Y et al: Cervical spondylosis: Evaluation of microstructural changes in spinal cord white matter and gray matter by diffusional kurtosis imaging. Magn Reson Imaging, 2014; 32: 428–32

5. Sun SW, Liang HF, Trinkaus K et al: Noninvasive detection of cuprizone induced axonal damage and demyelination in the mouse corpus callosum. Magn Reson Med, 2006; 55: 302–8

6. Poot DHJ, den Dekker AJ, Achten E et al: Optimal experimental design for diffusion kurtosis imaging. IEEE T Med Imaging, 2010; 29: 819–29

7. Wu EX, Cheung MM: MR diffusion kurtosis imaging for neural tissue characterization. NMR Biomed, 2010; 23: 836–48

8. Fukunaga I, Hori M, Masutani Y et al: Effects of diffusional kurtosis imaging parameters on diffusion quantification. Radiol Phys Technol, 2013; 6: 343–48

9. Fehlings MG, Tator CH: The relationships among the severity of spinal cord injury, residual neurological function, axon counts, and counts of retrogradely labeled neurons after experimental spinal cord injury. Exp Neurol, 1995; 132: 220–28

10. Jiang X, Ai C, Shi E et al: Neuroprotection against spinal cord ischemia-reperfusion injury induced by different ischemic postconditioning methods: Roles of phosphatidylinositol 3-kinase-Akt and extracellular signal-regulated kinase. Anesthesiology, 2009; 111: 1197–205

11. Zivin JA, Stashak J: The effect of ischemia on biogenic amine concentrations in the central nervous system. Stroke, 1983; 14: 556–62

12. Chen X, Zhu L, Wu G et al: A comparison between nucleus pulposus-derived stem cell transplantation and nucleus pulposus cell transplantation for the treatment of intervertebral disc degeneration in a rabbit model. Int J Surg, 2016; 28: 77–82

13. Lang-Lazdunski L, Heurteaux C, Mignon A et al: Ischemic spinal cord injury induced by aortic cross-clamping: Prevention by riluzole. Eur J Cardiothorac Surg, 2000; 18: 174–81

14. Liu B, Huang W, Xiao X et al: Neuroprotective effect of ulinastatin on spinal cord ischemia-reperfusion injury in rabbits. Oxid Med Cell Longev, 2015; 2015: 624819

15. Schwab JM, Brechtel K, Mueller CA et al: Experimental strategies to promote spinal cord regeneration – an integrative perspective. Prog Neurobiol, 2006; 78: 91–116

16. Crowe MJ, Bresnahan JC, Shuman SL et al: Apoptosis and delayed degeneration after spinal cord injury in rats and monkeys. Nat Med, 1997; 3: 73–76

17. Acute Y: Early acute management in adults with spinal cord injury: A clinical practice guideline for health-care providers. Who should read it? J Spianl Cord Med, 2008; 31: 403–79

18. Sribnick EA, Wingrave JM, Matzelle DD et al: Estrogen attenuated markers of inflammation and decreased lesion volume in acute spinal cord injury in rats. J Neurosci Res, 2005; 82: 283–93

19. Hinkle D, Baldwin S, Scheff S, Wise P: GFAP and S100beta expression in the cortex and hippocampus in response to mild cortical contusion. J Neurotraum, 1997; 14: 729–38

20. Nakanishi A, Fukunaga I, Hori M et al: Microstructural changes of the corticospinal tract in idiopathic normal pressure hydrocephalus: A comparison of diffusion tensor and diffusional kurtosis imaging. Neuroradiology, 2013; 55: 971–76

21. Zhu J, Wang X: [The study of correlation between age and anatomical segment in healthy lumbar interverbral discs by diffusion tensor imaging.] Chinese Journal of Magnetic Resonance Imaging, 2015; 6: 518–23 [in Chinese]

22. Ai C, Yan X, Jiang X et al: [Neuroprotective effects of modified ischemic postconditioning on spinal cord injury induced by ischemia reperfusion in rabbits.] Journal of China Medical University 2011; 40: 501–3 [in Chinese]

23. Wang YT, Lu XM, Zhu F et al: Ameliorative effects of p75NTR-ED-Fc on axonal regeneration and functional recovery in spinal cord-injured rats. Mol Neurobiol, 2015; 52: 1821–34

24. Tarlov I, Berman D, Moldaver J, Kellerman E: Regeneration of the cauda equina through nerve grafts: An experimental study in monkeys. AMA Arch Neurol Psychiatry, 1951; 65: 103–5

25. Li W, Huang D, Lyu Y: A comparative computational study of N-heterocyclic olefin and N-heterocyclic carbene mediated carboxylative cyclization of propargyl alcohols with CO2. Org Biomol Chem, 2016; 15: 3657–61

26. Chen X, Zhou C, Guo J et al: Effects of dihydroxylphenyl lactic acid on inflammatory responses in spinal cord injury. Brain Res, 2011; 1372: 160–68